RC #2: General comments

The paper "Evaluating critical rainfall conditions for large-scale landslides by detecting event times from seismic records" is a very interesting paper with original approach. The combination of the tools and methods to define rainfall threshold to landsliding is interesting and the several steps of the analysis are presented. However, the reader can be lost in the used databases, in particular between what concerns the 2009 typhoon analysis and the rest of the chronical. The results can be discussed (detection of only 62 landslides, thresholds between 500/300mm…), or justified by figures completed (see below comments on the figures).

R: The authors appreciate the constructive feedback of the reviewer – it has certainly helped the authors improve this manuscript. The reply is summarized as below:

1) Some confusing statements (e.g. landslide number, topic event, study period, etc.) will be modified in the revised manuscript.
2) The authors will provide and modify the description of data sources, quality, and accuracy (including rainfall information, satellite image, and seismic records).
3) More in-deep discussion on results will be added in the modified version.
4) The suggested modification of methods and figures will be done in the manuscript.

Specific comments:

1. **P2 L21: the event of 2009 is the only one mentioned, for the moment we can think that the research only focus on this event.**

R: The authors appreciate the reminding. We agree that the current manuscript may confuse readers due to many examples belonging to Typhoon Morakot. In the study, totally nineteen rainstorm events (seventeen typhoon-induced events and two heavy rainfall events) in the period of 2005-2014 were selected to examine the seismic records, but not only one event. The modified manuscript will clearly descript the targets in the section of introduction and study materials. The list of selected typhoons and heavy rainfall events will be added to the modified version (Table S2).

In the original manuscript, Typhoon Morakot was mentioned many times because it was one of the most tragic event in Taiwan in the past 20 years (more than 20,000 landslides, and more than four hundred large landslides with the disturbed area larger than 0.1 km^2), and therefore many good examples can be shown. In the modified version, the examples of other events will be added.

Table S2. List of selected nineteen rainstorm events (seventeen typhoons and two heavy rainfall events) to examine seismic records for identifying landslide-induced signals

	Event	Date (year/month/date)
1	Haitang	2005/07/16-07/20
2	Talim	2005/08/30-09/01
3	0609 Rain	2006/06/09
4	Bilis	2006/07/12-07/15
5	0604 Rain	2007/06/04
6	Kalmaegi	2008/07/16-07/18
7	Fung-Wong	2008/07/26-07/29
8	Sinlaku	2008/09/11-09/16
9	Morakot	2009/08/05-08/10
10	Fanapi	2010/09/17-09/20
11	Megi	2010/10/21-10/23
12	Nanmadol	2011/08/27-08/31
13	Talim	2012/06/19-06/21
14	Saola	2012/07/31-08/03
15	Tembin	2012/08/21-08/25
16	Soulik	2013/07/11-07/13
17	Trami	2013/08/20-08/22
18	Matmo	2014/07/21-07/23
19	Fung-Wong	2014/09/19-09/22

2. P3 L8: Date of the images? Number? Mapping only for the 2009 event.

R: Thanks for comments. The date and number of used SPOT-4 satellite images will be listed in Table S1. Landslide mapping was conducted for nineteen rainstorm events (seventeen typhoon-induced events and two heavy rainfall events).

3. P3 L23: Why 0.1km^2 Is it the limit of the automatic detection based on SPOT images? How many landslides were detected?

R: Based on the definition and characteristic of deep-seated gravitational slope deformation (DSGSD) and description of large-scale landslides (Lin et al., 2013; Lin et al., 2013), a large-scale landslide should have three characteristics, including 1) a depth larger than 10 m, 2) a volume greater than 1000,000 m^3, and 3) a speedy movement velocity. In practice, it is difficult to get these three characteristics without in-situ investigation and geodetic survey. Therefore, we chose the disturbed area of 100,000 m^2 (0.1 km^2, volume/depth) as the indicator to sort large-scale landslides from other types of slope failure. Landslide interpretation with satellite imagery is the fastest way to classify large-scale landslides. Actually, more than three hundred seismic signals

having the seismic characteristics of landslide-induced ground motions, however, only 62 signals having clear landslide-signal signatures were detected by at least three seismic stations. Therefore, we just could locate the possible locations of these 62 signals and paired the locating points with landslides. Although the successful detection and locating rate may be less than 20 % in the period of 2005-2014, we believe that the 62 landslides still provide many valuable time information.

Reference:

Lin, C. W., Tseng, C. M., Tseng, Y. H., Fei, L. Y., Hsieh, Y. C., and Tarolli, P. (2013). Recognition of large scale deep-seated landslides in forest areas of Taiwan using high resolution topography. Journal of Asian Earth Sciences, 62, 389-400.

Lin, M. L., Chen, T. W., Lin, C. W., Ho, D. J., Cheng, K. P., Yin, H. Y., and Chen, M. C. (2013). Detecting large-scale landslides using LiDar data and aerial photos in the Namasha-Liuoguey area, Taiwan. Remote Sensing, 6(1), 42-63.

4. **P3 L26: How we consider the progressive instability and the signal before the main failure?**

R: The authors agree that investigation of progressive instability is quite important. We believe that even slight displacement of materials on slope can stir energy transfer and induce seismic signals. However, the seismic signals generated by the processes of progressive deformation/displacement of material on slope do not contain enough energy to be recorded by remote seismic stations. Therefore, we did not try to monitor creeping processes by seismicity-approaches.

5. **P4 L3: Now we don't care about 2009 event. Why 2005-2014? What was the aim of 2009?**

R: Due to a large number of large landslides in 2009, the seismicity method for landslide-generated signals was successfully used. The study attempt to use the seismicity method for a longer period. Besides, the quality of seismic records of Taiwan's broadband seismic network had been significantly enhanced after 2005. The study period was decided to begin in 2005. In addition, identification of landslide-induced signals was conducted manually in the study. Therefore, identification cost a lot of time, and so far we finished the identification until 2014. So the study period during 2005-2004 was determined. It can be expected that more landslide signals will be found in the future.

6. **P4 L11: "only events with obvious signature", do you mean the 62 landslides in the fig.1? can you develop the characteristics of the signal that you can**

highlight with these 62 events?

R: The sentence maybe not clear. The revision is as below:

> "To reduce the uncertainty caused by the manual identification, the events with very obvious triangle-shape signatures in the spectrograms were used to examine rainfall statistics in this study."

The in-deep description of the characteristics of landslide-induced seismic signals will be added to text as follows:

> "…The seismic wave generated by landslide can be attributed to the shear force and loading on the ground surface as the mass moving downslope. Many studies have shown that the source mechanism of a landslide is highly complicated, and their seismic wave mainly consist of surface wave and shear wave, making it difficult to distinguish P wave and S wave from station records (Lin et al., 2010; Suwa et al., 2010; Dammeier et al., 2011; Feng, 2011; Hibert et al., 2014). The onset of landslide seismic signal is generally emergent. Then, the seismic amplitude increases gradually above ambient noise level to peak ground motion, exhibiting a 'cigar' shape envelope. After the peak amplitude, most of landslide-generated seismic signals have relatively long decay time, on average about 70% of total signal duration (Norris, 1994; La Rocca et al., 2004; Surinach et al., 2005; Deparis et al., 2008; Schneider et al., 2010; Dammeier et al., 2011; Allstadt, 2013). In frequency domain, landslide-induced seismic energy was mainly distributed below 10 Hz, with a triangular shaped signature in spectrogram, due to an increase over time in high-frequency constituents (Surinach et al., 2005; Dammeier et al., 2011)."

Reference:

Allstadt, K. (2013). Extracting source characteristics and dynamics of the August 2010 Mount Meager landslide from broadband seismograms. Journal of Geophysical Research: Earth Surface, 118(3), 1472-1490. doi:10.1002/jgrf.20110.

Dammeier, F., Moore, J. R., Haslinger, F., and Loew, S. (2011). Characterization of alpine rockslides using statistical analysis of seismic signals. Journal of Geophysical Research, 116(F4). doi:10.1029/2011jf002037

Deparis, J., Jongmans, D., Cotton, F., Baillet, L., Thouvenot, F., and Hantz, D. (2008). Analysis of rock-fall and rock-fall avalanche seismograms in the French Alps. Bulletin of the Seismological Society of America, 98(4), 1781-1796.

Doi:10.1785/0120070082.

Feng, Z. (2011). The seismic signatures of the 2009 Shiaolin landslide in Taiwan. Natural Hazards and Earth System Science, 11(5), 1559-1569. Doi:10.5194/nhess-11-1559-2011

Hibert, C., Ekström, G., and Stark, C. P. (2014). Dynamics of the Bingham Canyon Mine landslides from seismic signal analysis. Geophysical Research Letters, 41(13), 4535-4541. Doi:10.1002/2014gl060592

La Rocca, M., Galluzzo, D., Saccorotti, G., Tinti, S., Cimini, G. B., and Del Pezzo, E. (2004). Seismic signals associated with landslides and with a tsunami at Stromboli volcano, Italy. Bulletin of the Seismological Society of America, 94(5), 1850-1867. Doi:10.1785/012003238.

Lin, C. H., Kumagai, H., Ando, M., and Shin, T. C. (2010). Detection of landslides and submarine slumps using broadband seismic networks. Geophysical Research Letters, 37(22), n/a-n/a. doi:10.1029/2010gl044685

Norris, R. D. (1994). Seismicity of rockfalls and avalanches at 3 Cascade Range volcanos – Implications for seismic detection of hazardous mass movements. Bulletin of the Seismological Society of America, 84(6), 1925-1939.

Schneider, D., Bartelt, P., Caplan-Auerbach, J., Christen, M., Huggel, C., and McArdell, B. W. (2010). Insights into rock-ice avalanche dynamics by combined analysis of seismic recordings and a numerical avalanche model. Journal of Geophysical Research, 115(F4). Doi:10.1029/2010jf001734.

Surinach, E., Vilajosana, I., Khazaradze, G., Biescas, B., Furdada, G., and Vilaplana, J. M. (2005). Seismic detection and characterization of landslides and other mass movements. Natural Hazards and Earth System Sciences, 5, 791-798.

Suwa, H., Mizuno, T., and Ishii, T. (2010). Prediction of a landslide and analysis of slide motion with reference to the 2004 Ohto slide in Nara, Japan. Geomorphology, 124(3-4), 157-163. Doi:10.1016/j.geomorph.2010.05.003.

7. P4 L19: how can you consider the lag time between rainfall / soil saturation… and failure?

R: Thanks for the valuable comments. This study used seismic signals to find out landslide occurrence time, and undoubtedly this time information could help to study the infiltration of rainfall or the relationship between soil saturation and landslides. However, this study currently focused on constructing and compare the rainfall thresholds for landslide warning, the traditionally statistical methods to estimate rainfall threshold were chosen. Time lag between rainfall history and soil saturation process was not considered in the study.

8. P4 L29: I think the chosen method can be shortly developed here.

R: Thanks for t your suggestion. The detailed content of locating method will be added to the text as follows:

> "…. Locations are estimated with a cross-correlation method that could maximizes tremor signal coherency among seismic stations. The criteria of station chosen was based on geographic distribution and tremor signal-to-noise ratios. The interpreted signals would be created envelope function to process cross-correlation analyzed from different station pairs. We obtain centroid location estimates by cross-correlating all station pairs and performing the Monte Carlo grids searching method (Wech and Creager, 2008). While traditional methods seek the source location that minimizes the horizontal time difference between predicted travel time and peak lag time, the method seek to minimize the vertical correlation distance between the peak correlation value and the predicted correlation value."

Reference:

Wech, A. G., and Creager, K. C. (2008). Automated detection and location of Cascadia tremor. Geophysical Research Letters, 35(20).

9. P4 L35: there is only Xiaolin landslide in this figure. So you focus on 2009 events? do you compared all the landslides detected by remote sensing (fig.1 is it landslides detected by seismic signal of remote sensing: to clarify) (how many by remote sensing?) with the seismic signal? an example of signal related to a smaller event than Xiaolin would be interesting (fig.3). Do the SSLs have a significant signal also?

R: Thanks for the comments. In the figure 2c, six matched landslides (including Xiaolin) were visible. Each orange circle means a successfully-paired landslide. The outline of each paired landslide will be added to the figure. Besides, the signal and spectrogram of a 2005 large landslide smaller than Xiaolin will be provided and added to modified manuscript as below:

Theoretically, the seismic signal induced by a small landslide could be found if there is a seismic station very close to it. In practice, the seismic signals generated by small landslides do not contain enough energy to be recorded by remote seismic stations. Therefore, we do not try to examine small landslides by seismicity approaches.

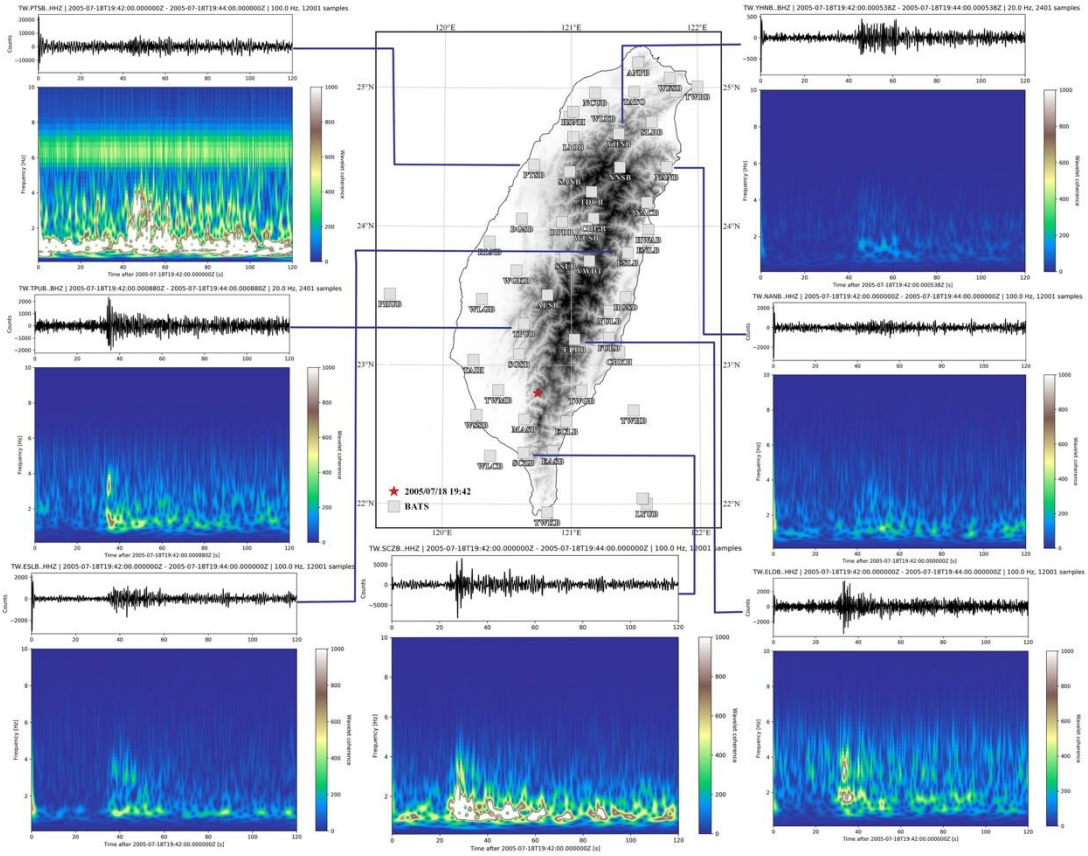

10. P5 L3: Now you are studying events between 2005-2014? It is a little bit confusing. How many typhoon events? don't you consider previous smaller rainfall events that could affect the mechanical properties of the slopes?

R: In the study, totally seventeen typhoon events and two heavy rainfall events occurring in the period of 2005-2014 were chosen to examine the seismic records and identify landslide-induced signals. The list of selected events will be provided in Table S2.

In the study, seven-days antecedent rainfall was considered as a rainfall parameter. The effect of antecedent rainfall should decay with time. Therefore, decay rate of antecedent rainfall with day was used to estimate effective rainfall. According to the decay rate, 0.7, the effect of antecedent rainfall with counting days longer than 7 days is slight. In the study, we adopt seven-days antecedent rainfall to estimate effective rainfall.

Table S2

	Event	Date (year/month/date)
1	Haitang	2005/07/16-07/20
2	Talim	2005/08/30-09/01
3	0609 Rain	2005/06/09
4	Bilis	2005/07/12-07/15

5	0604 Rain	2006/06/04
6	Kalmaegi	2006/07/16-07/18
7	Fung-Wong	2008/07/26-07/29
8	Sinlaku	2008/09/11-09/16
9	Morakot	2009/08/05-08/10
10	Fanapi	2010/09/17-09/20
11	Megi	2010/10/21-10/23
12	Nanmadol	2011/08/27-08/31
13	Talim	2012/06/19-06/21
14	Saola	2012/07/31-08/03
15	Tembin	2012/08/21-08/25
16	Soulik	2013/07/11-07/13
17	Trami	2013/08/20-08/22
18	Matmo	2014/07/21-07/23
19	Fung-Wong	2014/09/19-09/22

11. P5 L6: How can you consider the topographic, orographic effects?

R: We appreciate the comments. We tested the rainfall data used in the study to validate the influence of distance and topographic effect on rainfall distribution. The effect of rain gauge distribution over the accuracy of rainfall has been assessed using gauge observation in a 35 km × 50 km region of south Taiwan (Fig. S1). The amounts of daily rainfall during 2009 Typhoon Morakot (8/6-8/11) recorded at 19 rain gauge stations were selected to validate the accuracy of rainfall. The influence of topography on rainfall variability has been analyzed in the same 35 km × 50 km region of south Taiwan. The highest station elevation is 1792 m a.s.l. at C1V270, and the lowest station elevation is 105 m a.s.l. at C10830. The standard deviation of station elevation is 561 m. The values of standard deviation of daily rainfall at the 19 stations were calculated, and less than 13% except a high standard deviation, 45%, on sixth August (average daily rainfall less than 2 mm). The results demonstrated that high and even extreme rainfall are less influenced by elevation, while low and medium rainfall events are significantly influenced by elevation variation, with most of the rainfall appearing on high elevations. Similar results have also been reported by some previous studies (Sanchez-Moreno et al., 2014; Ge et al., 2017). Because the study only considered the rainfall events with total cumulated rainfall greater than 500 m, the elevation effect was ignored as selecting rain station.

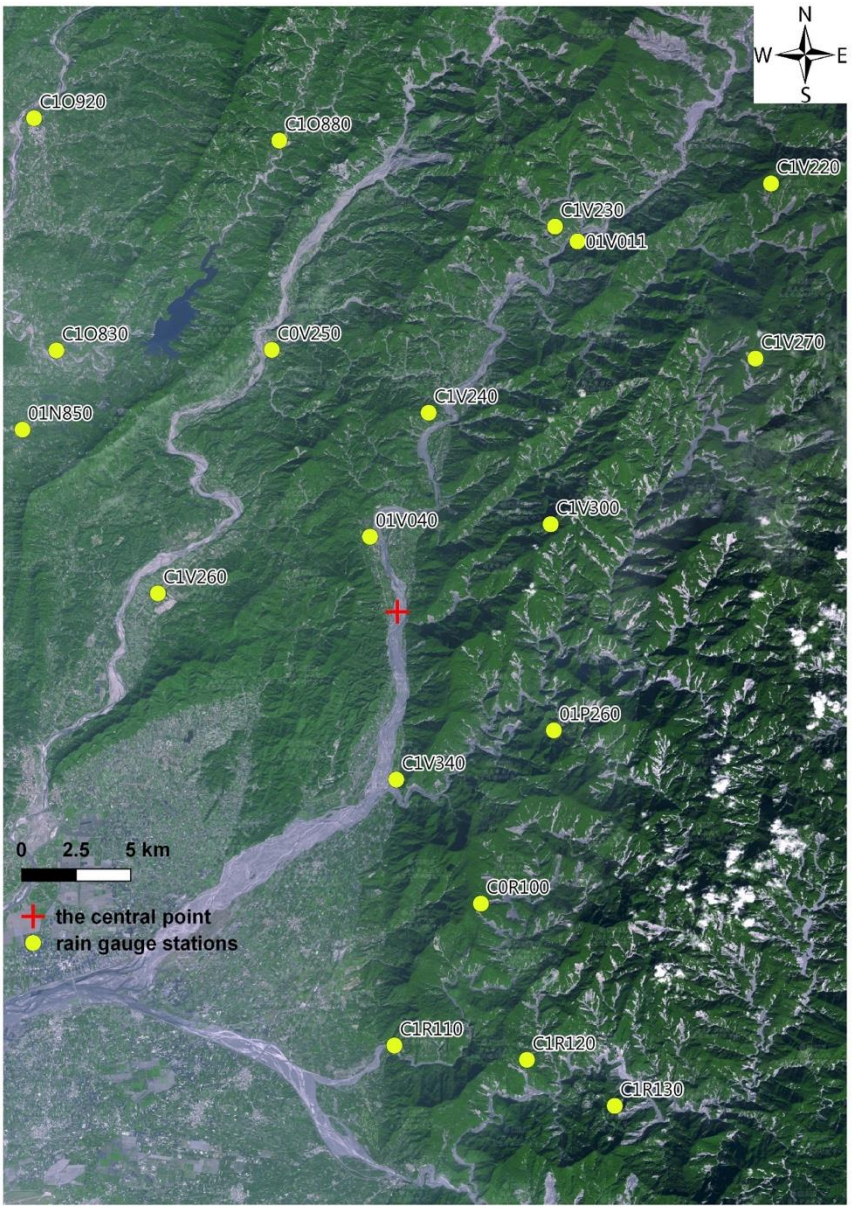

Fig. S1. The distribution of rain gauge stations and the location of the central point of the testing area for validating the influence of the distance between rain gauge and a given point.

Reference:

Sanchez-Moreno, J.F., Mannaerts, C.M., and Jetten, V. (2014) Influence of topography on rainfall variability in Santiago Island, Cape Verde. International Journal of Climatology, 34, 1081-1097.

Ge, G., Shi, Z., Yang, X., Hao, Y., Guo, H., Kossi, F., Xin, Z., Wei, W., Zhang, Z., Zhang, X., Liu, Y., and Liu, J. (2017) Analysis of Precipitation Extremes in the

Qinghai-Tibetan Plateau, China: Spatio-Temporal Characteristics and Topography Effects. Atmosphere, 8(7), 127, doi:10.3390/atmos8070127.

12. P5 L10: 100km² is already large catchment.

R: The effect of station distance has been tested to variation of rainfall. The errors of daily rainfall between the central point and the nearest rain gauge station (01V040) were smaller than 10 % (0.5%-10% at different date). Besides, the correlation coefficients would keep at 90% as a distance between the central point and rain gauge stations less than 20 km, and even keep at 98% as a distance less than 10 km (Fig. S2). Therefore, in the study, an upper limit of basin area smaller than 100 km^2 (10 km × 10 km was adopted to avoid a significant decrease of the accuracy of rainfall. Because the density of rainfall stations in mountainous area would significantly decreases, the number of usable rainfall stations may be limited. The size of catchment area of 100km^2 is the upper limit for choose rainfall station. In practice, we chose the closest rainfall station.

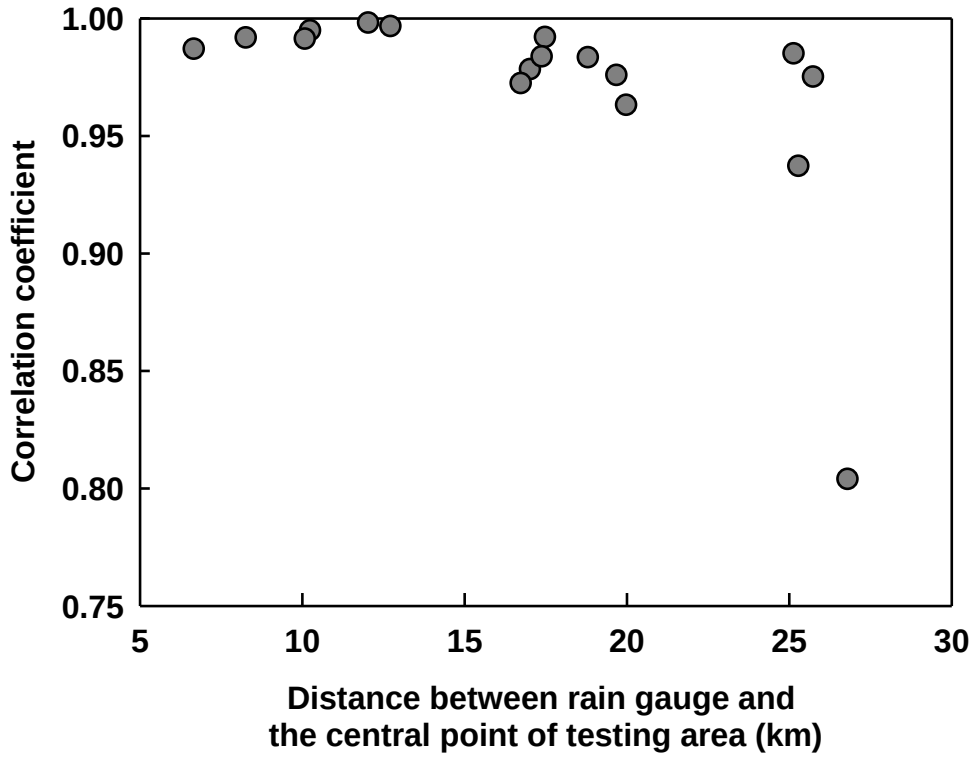

Fig. S2. Variation of correlation coefficient

13. P5 L2: rain event = typhoon?

R: Yes. The sentence will be revised.

14. P6 L4: 193 small landslides for which period?

R: The 193 small landslides were investigated by SWBC during 2006-2013. The illustration on the small landslides will be improved in the later version of manuscript.

15. P6 L15: EQ1 cohesion here is only considered for a discontinuity (C = 0)? Or for the specific material?

R: We thanks reviewer's recommendation. Well development of detachment plane (e.g., sliding surface between sedimentary layers, connected joints, weathered foliation, etc.) have been widely considered as one important geological condition to induce a large landslide. Therefore, in the study, the C' of the detachment plane is simply assumed as the value of zero to behave the critical situation of slope stability. Cohesion in equation (1) is not considered for a specific material. The illustration of C' will be modified in the text.

> "…Well development of detachment plane (e.g., sliding surface between sedimentary layers, connected joints, weathered foliation, etc.) have been widely considered as the geological conditions to occur a large landslide (Agliardi et al., 2001; Tsou et al., 2011)."

Reference:

Tsou, C. Y., Feng, Z. Y., & Chigira, M. (2011). Catastrophic landslide induced by typhoon Morakot, Shiaolin, Taiwan. Geomorphology, 127(3-4), 166-178.

Agliardi, F., Crosta, G., & Zanchi, A. (2001). Structural constraints on deep-seated slope deformation kinematics. Engineering Geology, 59(1-2), 83-102.

16. P7 L9/22: lower slopes VS steeper slopes… upslope VS downslope? Can you explain it? Is it a regressive erosion of the slope?

R: Thanks for the important reviewing. The sentence should be revised as below:

> "…due to the fact that during the extremely heavy rainfall of Typhoon Morakot in 2009, more than 2,000 mm precipitated in four days, causing a large number of landslides, and exhausting a lot of unstable slopes. Consequently, landslides transferred to occur on steeper slopes in the following years."

17. P7 L9/24 & 26: landslides for 2009 event? Or the detection of 62 landslides grounded on seismic signal among 686 inventoried landslides? What is the landslide seismic magnitude?

R: In this section, the topographic analysis was for 686 large landslides during 2005-2014. The paragraph will be modified to avoid confusion. We did not calculate landslide

seismic magnitude in the study due to the lack of a standard method for estimating landslide seismic magnitude so far.

18. P8 L4: what about SSL?

R: Most of the small landslides have strong instantaneous rainfall intensity. This means that a short duration and heavy rainfall can easily trigger small landslides.

Discussion:

The discussion is interesting because it puts the results in perspective. Nevertheless, some points have to be clarify.

19. 5.1. The authors highlight the fact that critical rainfall to trigger landslides has decreased since 2010 (500mm to 300mm) according to the results fig. 7. How many events the threshold is based on? The figure 7 is not so evident.

To explain these results, the authors question the Morakot typhoon. Was it an exceptional hydro-climatic event? The other solution is that instabilities induced by the 2009 typhoon are responsible of recent landslides. This idea should be developed here, and maybe associated to a map of the landslides scars (delineation of the departure areas) and differentiated according to the periods of the triggering…

R: Thanks for comments. The authors agree the conceptual view of reviewer. The discussion needs more solid information and field investigation. Therefore, the part about the influence of rock types and an extreme event will be removed and replaced with in-deep comparison of different rainfall threshold.

20. 5.2. The authors mention the fact that landslides occurred several types of rocks with different geotechnical behaviors, but the chosen geotechnical parameters (table 1) are identical. Why?

R: The main research purpose of this study was to establish a rainfall warning threshold which is applicable for large landslides, so a relatively simple but effective method was adopted. In this method, Keefer (1987) assumes that there is a potential sliding surface for these landslides, and the depth of the large-scale landslides are often deep to the strata. Therefore, although the movements of the soil material are not completely the same, under this assumption, it can still reach a considerable good effect.

In order to improve the Qc threshold, the critical volume of water, Q_c, for each large landslide was estimated based on its slope gradient and depth (estimated by the equation: $Z = 26.14A^{0.4}$; Z: depth, m; A: disturbed area, m^2). Following the equation (4), the drainage rate, $I_{0,}$ for each landslide can be calculated. For the 62 detected landslide, the cumulative probability of 5% of Q_c and I_0 values was taken as the critical values in the

mixing physically- and statistically-based threshold. The critical value of I_0 was 1.5, and the critical Qc was 430.2. The paragraph will be modified as follows:

> "The critical volume of water, Q_C, on sliding surface for each large landslide was estimated based on its slope gradient, depth (estimated by the equation: $Z = 26.14A^{0.4}$; Z: depth in m; A: disturbed area in m^2), and the geological material parameters of the study area (Table 1). The Q_C value was inserted into $Q_C = (I - I_0) \cdot D$ to obtain an I_0 value for each large landslide. For the 62 detected landslide, the cumulative probability of 5% of Qc and I_0 values was taken as the critical values. The critical value of I_0 was 1.5, and the critical Q_C was 430.2, which is more suitable for LSLs than for SSLs, and the threshold curve was rewritten as $(I - 1.5) \cdot D = 430.2$."

21. Effective rainfall, and rainfall duration thresholds according to the rock types are not clear in the figure 8, could another statistical analysis put the conclusion of the authors in obvious fact?

R: Thank you for your suggestion. The figure will be removed.

Figure:

22. Fig. 2. Add legend for the detected landslide: Is it detected by seismic signal analysis? Is the point, the centroid of the landslide? Why not the delineation of the landslide body? Dates of the both satellite images here.

R: Thank you for your suggestion. The figure will be modified based on suggestions.

23. Fig. 3. Location of the detected landslides in 2009? Is there other spectrogram for previous landslides? Or after 2009? or associated to another landslide triggered in 2009: X spectrogram for 1 landslide. The star is the location defined with which seismic station?

R: This events, the Xioulin landslide, is one of the most tragic event during Typhoon Morakot, 2009. The other 61 detected landslides also have the triangle-shape characteristic patterns in their spectrograms. The star is the location defined with all the stations which could detect the signals from the Xioulin landslide. We will provide two examples of spectrograms of one landslide in 2005 and one landslide after 2009 in supplementary materials.

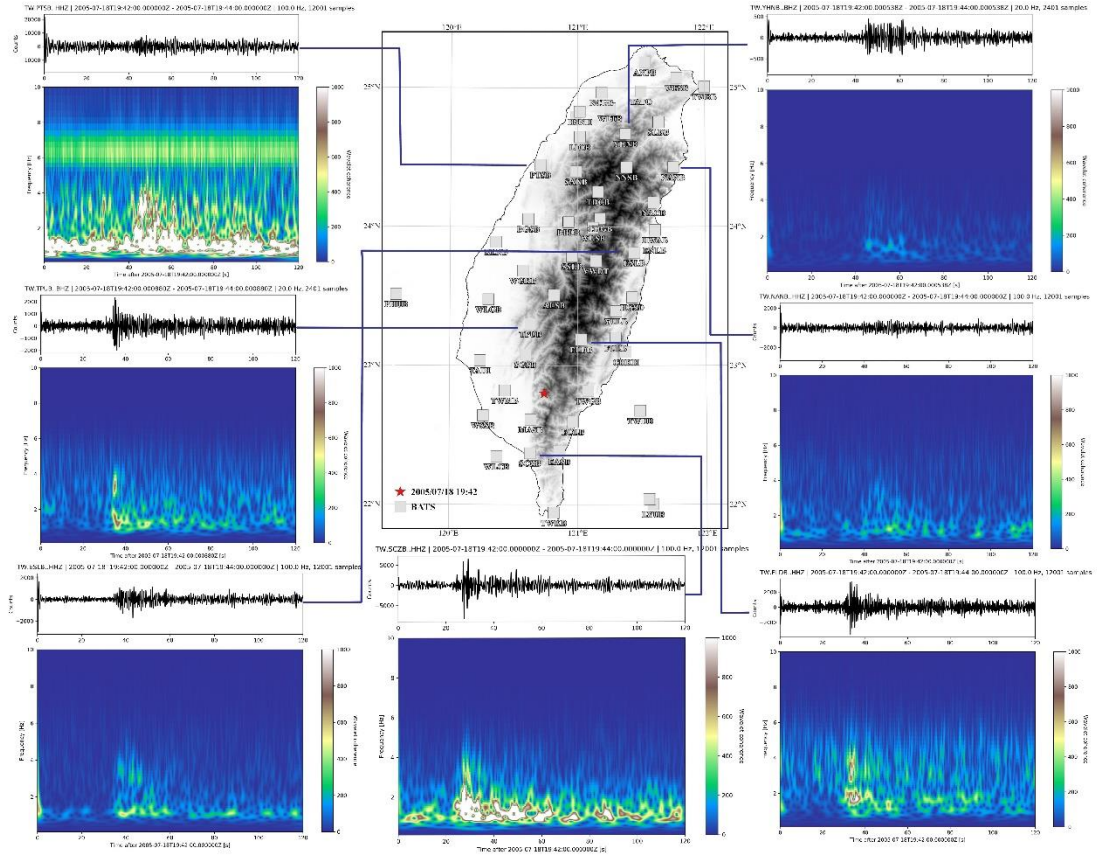
2005/07/18 19:42
BATS

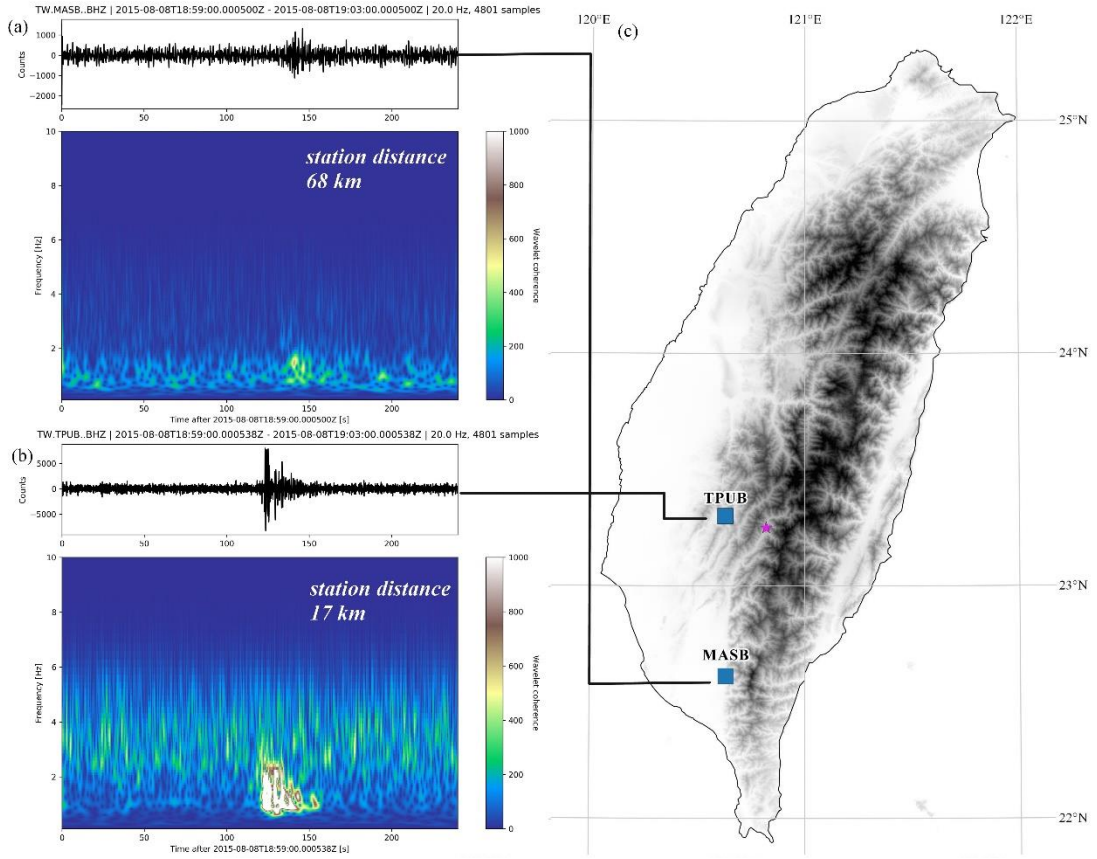
(a)
TW.MASB..BHZ | 2015-08-08T18:59:00.000500Z - 2015-08-08T19:03:00.000500Z | 20.0 Hz, 4801 samples
Counts
station distance
68 km
Frequency [Hz]
Wavelet coherence
Time after 2015-08-08T18:59:00.000500Z [s]
(b)
TW.TPUB..BHZ | 2015-08-08T18:59:00.000538Z - 2015-08-08T19:03:00.000538Z | 20.0 Hz, 4801 samples
station distance
17 km
Time after 2015-08-08T18:59:00.000538Z [s]
(c)
120°E
121°E
122°E
25°N
24°N
23°N
22°N
TPUB
MASB

24. Fig. 4. Maybe with the topography visible on the map?

R: Thank you for your suggestion. We had tried added topography in the fig. 4a. However, so many information made visually chaotic.

25. Fig. 7. A) Is there only 1 event for the lowest limit?

R: Yes. The figure will be removed in modified version.

Table S1

	Date and time (UTC)	Longitude	Latitude	Disturbed area (km^2)	Elev. of Landslide (m)	Rain Station	Distance (km)	Elev. of Rain station (m)	Reactive Landslide	Image Date
1	2005/07/18 19:42	120.74	22.80	0.13	1388.6	C1R120	5.3	820	N	2005/07/25
2	2005/07/20 18:15	120.75	22.74	0.13	813.7	C1R130	0.9	1040	N	2005/07/25
3	2005/07/20 21:55	120.82	22.88	0.12	1535.0	01P260	10.8	458	N	2005/07/25
4	2005/07/21 06:33	120.72	22.85	0.18	950.1	C0R100	3.9	1006	R	2006/07/29
5	2006/06/09 16:53	121.33	24.29	0.11	2304.6	C1H860	24.1	1840	R	2006/07/19
6	2008/07/18 21:30	121.01	23.82	0.10	1093.8	C1I040	1.6	1693	R	2008/11/20
7	2008/07/18 23:55	120.66	23.15	0.12	749.0	C1V230	6.0	760	N	2008/11/25
8	2008/09/15 02:45	121.38	24.35	0.14	2236.4	41U090	5.7	1930	R	2008/12/03
9	2008/09/17 18:50	121.00	24.10	0.89	1104.3	01F100	2.6	1600	N	2008/11/15
10	2009/08/08 00:04	120.72	22.57	0.39	1207.1	C1R240	10.9	74	R	2010/04/10
11	2009/08/08 00:35	120.73	22.49	0.12	950.2	01Q350	6.2	700	N	2010/04/10
12	2009/08/08 01:20	120.77	23.49	0.14	1411.2	H1M240	5.2	1850	N	2010/02/23
13	2009/08/08 02:20	120.85	22.98	0.11	2167.4	01P260	15.2	458	R	2010/04/10
14	2009/08/08 03:55	120.75	23.08	0.33	923.5	C1V270	5.4	1792	R	2010/02/23
15	2009/08/08 05:35	120.83	23.52	0.50	1903.4	C0H9A0	2.4	1595	N	2010/02/23
16	2009/08/08 06:25	120.82	23.06	0.39	1726.3	01V040	20.8	265	N	2010/02/23
17	2009/08/08 06:28	120.67	23.01	0.15	517.2	01V040	4.0	265	N	2010/02/23
18	2009/08/08 07:15	120.70	23.01	0.23	903.9	C1V300	1.5	1637	N	2010/02/23
19	2009/08/08 07:35	120.70	22.75	0.49	647.8	C1R120	1.0	820	R	2010/02/23
20	2009/08/08 08:10	120.81	23.00	0.19	2007.5	C1V300	10.1	1637	R	2010/02/23
21	2009/08/08 08:20	120.91	23.33	0.41	1703.8	01V070	6.3	2230	N	2010/01/11
22	2009/08/08 09:01	120.79	22.61	0.62	1222.0	01Q910	13.4	1158	R	2010/04/10

23	2009/08/08 10:40	120.86	22.80	0.16	1424.2	01Q910	12.8	1158	R	2010/04/10
24	2009/08/08 11:35	120.95	23.33	0.22	2029.6	C1V170	15.1	3340	N	2010/01/11
25	2009/08/08 13:56	120.66	22.96	0.11	407.3	01V040	5.0	265	N	2010/02/23
26	2009/08/08 16:15	120.88	23.18	0.14	2162.1	C1V220	7.4	1781	R	2010/01/11
27	2009/08/08 17:05	120.71	22.49	0.94	1168.5	C1R240	9.3	74	N	2010/04/10
28	2009/08/08 17:21	120.90	23.07	0.28	2606.3	C1V270	9.8	1792	R	2010/04/10
29	2009/08/08 17:53	120.91	23.08	0.19	2459.5	C1V270	10.7	1792	R	2010/04/10
30	2009/08/08 18:11	120.79	23.51	1.12	1763.8	467530	2.8	2413.4	N	2010/02/23
31	2009/08/08 18:16	120.83	22.63	0.72	1055.7	01Q910	13.5	1158	R	2010/04/10
32	2009/08/08 18:19	120.72	22.70	0.56	603.4	01Q910	5.3	1158	R	2010/03/06
33	2009/08/08 18:28	120.66	22.95	0.12	554.4	01V040	5.8	265	R	2010/02/23
34	2009/08/08 19:19	120.71	22.67	0.64	705.7	01Q910	7.6	1158	R	2010/03/06
35	2009/08/08 20:15	120.73	22.59	0.73	1509.7	C1R240	12.8	74	N	2010/04/10
36	2009/08/08 20:27	120.92	23.40	0.12	2278.6	C1V460	4.5	1949	N	2010/01/11
37	2009/08/08 21:11	120.90	23.46	0.15	1904.4	C1V460	2.3	1949	R	2010/02/23
38	2009/08/08 21:30	120.92	23.49	0.12	2450.4	C1V460	6.4	1949	N	2010/02/23
39	2009/08/08 21:42	120.91	23.10	0.25	2274.1	C1V460	37.3	1949	R	2010/04/10
40	2009/08/08 22:16	120.66	23.17	2.50	681.3	C1R880	6.4	223	R	2010/02/23
41	2009/08/08 22:52	120.90	23.54	0.12	1936.8	C1I340	4.5	897	R	2010/02/23
42	2009/08/08 23:02	120.60	23.03	0.13	747.9	C0V250	5.2	298	N	2010/04/10
43	2009/08/08 23:14	120.75	23.29	0.56	1525.1	C1V200	7.7	860	R	2010/02/23
44	2009/08/08 23:15	120.77	22.63	0.15	2309.0	01Q250	8.2	950	R	2010/04/10
45	2009/08/08 23:41	120.84	22.63	0.12	825.0	01Q910	13.9	1158	R	2010/04/10
46	2009/08/09 00:34	120.77	23.22	2.24	1352.5	C1V210	4.0	700	R	2010/02/23
47	2009/08/09 02:52	120.77	23.23	0.81	1559.3	C1V210	4.1	700	R	2010/02/23
48	2009/08/09 03:55	120.72	22.60	0.63	923.5	01Q250	2.5	950	N	2010/04/10
49	2009/08/09 09:37	120.81	22.56	2.31	1144.3	01Q350	14.3	250	N	2010/04/10

50	2009/08/09 11:00	120.77	22.82	0.13	1669.4	C1R120	9.0	820	R	2010/04/10
51	2009/08/10 03:54	120.80	23.25	0.20	1227.6	C1V210	2.8	700	R	2010/02/23
52	2009/08/10 04:22	120.76	23.31	1.52	1387.2	C1V160	6.3	1040	R	2010/02/23
53	2010/09/19 23:24	120.73	22.85	0.15	1135.0	01Q910	13.9	1158	R	2011/04/16
54	2011/08/30 07:10	120.93	22.86	0.12	849.8	01Q350	44.9	1275	R	2012/02/27
55	2011/08/30 09:13	121.18	23.69	0.11	1811.5	C1T940	19.6	1570	R	2012/02/27
56	2011/08/31 09:37	120.98	23.33	0.11	2714.0	01V070	8.5	2230	R	2012/02/27
57	2012/08/01 18:40	121.42	24.58	0.12	1512.0	01U050	8.1	400	R	2013/07/11
58	2012/08/02 10:00	121.85	24.52	0.12	83.3	C0U710	33.3	1810	N	2013/06/28
59	2012/08/02 19:00	120.95	23.74	0.25	1677.9	C1I310	6.6	1001	N	2013/06/03
60	2012/08/03 01:02	121.38	24.36	0.19	2356.6	41U090	4.7	1930	N	2013/07/11
61	2013/07/13 14:27	120.89	23.02	0.40	2604.8	C1V270	10.1	1792	R	2014/07/13
62	2013/08/22 19:05	121.07	23.38	0.18	2114.6	C1I140	41.2	1700	R	2014/07/13